

Supplementary Material

Structure, energetics and thermodynamics of PLGA condensed phases from Molecular Dynamics

James Andrews^{a,b,1}, Robert A. Handler^{a,c,2}, Estela Blaisten-Barojas^{a,b,3,*}

^a*Center for Simulation and Modeling (former Computational Materials Science Center),*

^b*Department of Computational and Data Sciences,*

^c*Department of Mechanical Engineering,
George Mason University, Fairfax, Virginia 22030, USA*

Keywords: poly(lactic-co-glycolic acid) (PLGA), glass transition, response
thermodynamic properties, caloric curve, solid-state stability

1. PLGA atomic charges

Fourteen models of RESP atomic charges were calculated for different structures of extended PLGA(50:50) chains with 24 monomers each, illustrated in Fig. S1. The alternation of lactic acid (L) and glycolic acid (G) in each oligomer is random. The obtained sequence of Ls and Gs for each of the models depicted in Fig. S1 is given in Table S1.

Larger chains with 90, 156, 222 and 310 monomers were built using the 22 internal monomers of the above models for central portions and 23 monomers for ending the polymer chains. Each PLGA(50:50) is ended by a lactic acid on one end and a glycolic acid on the other end. Table S2 indicates the models that have entered in the construction of these longer chains.

2. Energy properties

*Corresponding author: blaisten@gmu.edu (Estela Blaisten-Barojas)

¹Orcid=0000-0002-0498-1665

²Orcid=0000-0001-5263-3967

³Orcid=0000-0003-3259-1573

Table S 1: Sequence of lactic acid and glycolic acid monomers in the PLGA(50:50) oligomers with 24 monomers. The enantiomers of the lactic acid are L and D. The glycolic acid is G.

1	LGDDGGGLGGGLGDGLDDGGLDLG
2	LGGGLDDGGGLDGGLGDGDGLDG
3	LGDLGGDDGDDLGGLGDGGGLGG
4	LGLLGGGGDDGGDGLDDLGGDLG
5	LGGGGGLGGDGDGDLLDGLGDDLG
6	LGGLLDGGDGGDGDGDDGLDLDLG
7	LGDGDLGGGLLGGDDGDGGDLG
8	LGDGDDGGGGGLDLGLDGGLGLG
9	LGGLGLGDGDGLGDDGGLDGLG
10	LGGDDGGLGDDGLDGLGDGGGLG
11	LGDGDGGGDDGGGLDLGLDGGLG
12	LGGDDDLGLDLGDGGGGDLGGGLG
13	LGDGDGLGGDGGLDDLGGLDGLG
14	LGGGGGDDGGGDLLGDLGDDLG

Table S 2: The 24-mer models that stitched together formed longer PLGA(50:50) chains

90	1, 2, 3, 4
156	8, 9, 10, 11, 12, 13, 14
222	14, 13, 12, 11, 10, 9, 8, 5, 4, 3
310	1, 2, 3, 4, 5, 6, 7, 8, 9, 10, 11, 12, 13, 14

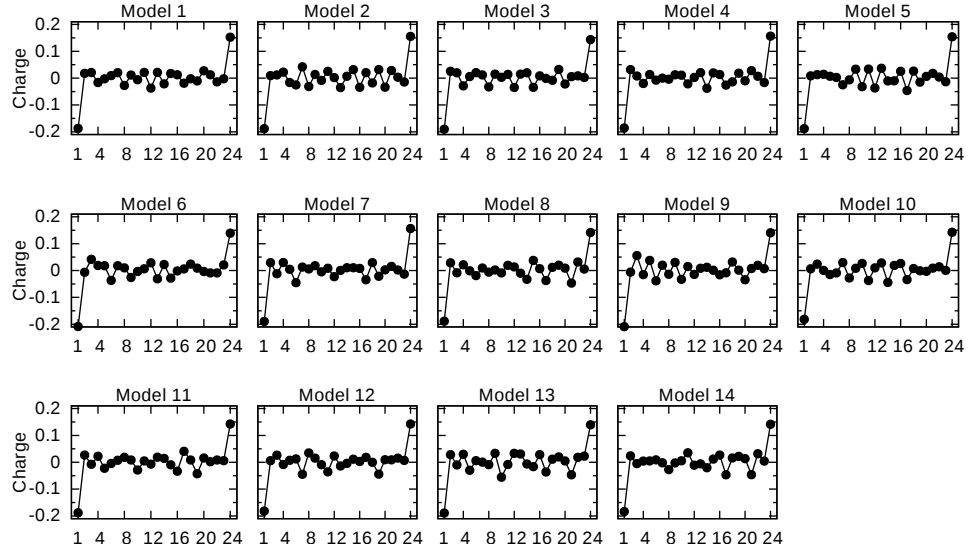


Figure S 1: RESP charges in units of e for each of the monomers in the 14 different PLGA(50:50) oligomers considered.

The path to equilibrium was analyzed in detail for every simulation. Reported values in tables do not include the previous equilibration history of the system. Example of such previous equilibration history is provided in Fig. S2 that shows a coarse grained time average of the density as a function of time at $T=500$ K and 1 atm for 156-PLGA, RESP case. The figure shows how the system evolves from a state of low density to the final state.

Table S3 provides the energetics of the PLGA(50:50) condensed systems at low and high temperatures from 20 ns of MD-NVE simulations.

3. Determination of the glass transition of condensed PLGA(50:50)

Figure S3 provides a visual inspection of the two methods used for determining the glass transition for the RESP case: (i) in left panes the Legendre transform of the enthalpy H as a function of temperature T for the five PLGA(50:50) condensed systems considered and (ii) in central panes the determination form the fluctuations of the enthalpy σH . Panes at the right of Fig. S2 identify the

Table S 3: Energy properties at T=200 K, T=400 K, and T=500 K and at their equilibrium densities for the RESP and BCC cases. Total potential energy/monomer ($E_{total/mer}$), sum of chain potential energies/monomer ($E_{intra/mer}$), cohesive energy E_{coh} , sample volume, cohesive energy density (e_{coh}), Hildebrand solubility parameter (δ_h).

		RESP				
		24	90	156	222	310
$T = 200\text{ K}$	$E_{total/mer}$ (kJ/mol)	46.5 \pm 0.1	48.1 \pm 0.1	48.3 \pm 0.1	48.0 \pm 0.1	48.1 \pm 0.1
	$E_{intra/mer}$ (kJ/mol)	77.0 \pm 0.1	70.9 \pm 0.1	68.9 \pm 0.1	67.0 \pm 0.1	64.1 \pm 0.1
	E_{coh} (MJ/mol)	79.0 \pm 0.1	65.8 \pm 0.1	51.3 \pm 0.1	50.5 \pm 0.1	44.5 \pm 0.1
	V (nm ³)	211.1	233.8	202.5	215.6	225.6
	e_{coh} (MPa)	622 \pm 1	467 \pm 1	421 \pm 1	389 \pm 1	328 \pm 1
	δ_h (MPa ^{1/2})	24.9 \pm 0.02	21.62 \pm 0.02	20.52 \pm 0.03	19.72 \pm 0.02	18.10 \pm 0.02
$T = 400\text{ K}$	$E_{total/mer}$ (kJ/mol)	67.5 \pm 0.2	68.8 \pm 0.1	69.1 \pm 0.1	68.7 \pm 0.2	68.7 \pm 0.2
	$E_{intra/mer}$ (kJ/mol)	94.4 \pm 0.2	89.2 \pm 0.16	87.3 \pm 0.2	85.6 \pm 0.2	82.9 \pm 0.2
	E_{coh} (MJ/mol)	69.7 \pm 0.2	58.7 \pm 0.2	45.4 \pm 0.2	45.0 \pm 0.3	39.7 \pm 0.2
	V (nm ³)	223.516	246.591	214.131	227.645	238.091
	e_{coh} (MPa)	518 \pm 2	395 \pm 2	352 \pm 2	329 \pm 2	277 \pm 1
	δ_h (MPa ^{1/2})	22.75 \pm 0.04	19.89 \pm 0.04	18.77 \pm 0.04	18.12 \pm 0.06	16.65 \pm 0.04
$T = 500\text{ K}$	$E_{total/mer}$ (kJ/mol)	80.8 \pm 0.2	80.8 \pm 0.2	81.0 \pm 0.2	80.8 \pm 0.2	80.9 \pm 0.2
	$E_{intra/mer}$ (kJ/mol)	104.5 \pm 0.2	99.1 \pm 0.2	97.2 \pm 0.2	95.2 \pm 0.2	94.0 \pm 0.2
	E_{coh} (MJ/mol)	61.3 \pm 0.4	52.7 \pm 0.35	40.5 \pm 0.5	38.5 \pm 0.4	35.6 \pm 0.4
	V (nm ³)	237.3	260.0	225.75	239.9	251.2
	e_{coh} (MPa)	429 \pm 3	337 \pm 2	298 \pm 3	267 \pm 2	236 \pm 2
	δ_h (MPa ^{1/2})	20.71 \pm 0.07	18.35 \pm 0.06	17.26 \pm 0.10	16.33 \pm 0.07	15.35 \pm 0.08
		BCC				
		24	90	156	222	310
$T = 200\text{ K}$	$E_{total/mer}$ (kJ/mol)	20.1 \pm 0.1	22.6 \pm 0.1	23.4 \pm 0.1	23.4 \pm 0.1	23.6 \pm 0.1
	$E_{intra/mer}$ (kJ/mol)	54.4 \pm 0.1	47.3 \pm 0.1	45.2 \pm 0.1	43.3 \pm 0.1	43.6 \pm 0.1
	E_{coh} (MJ/mol)	88.8 \pm 0.1	71.1 \pm 0.1	54.3 \pm 0.1	53.1 \pm 0.1	55.6 \pm 0.1
	V (nm ³)	209.4	231.2	200.9	214.2	224.5
	e_{coh} (MPa)	704 \pm 1	511 \pm 1	449 \pm 1	412 \pm 1	411 \pm 1
	δ_h (MPa ^{1/2})	26.54 \pm 0.02	22.60 \pm 0.02	21.19 \pm 0.02	20.29 \pm 0.02	20.28 \pm 0.02
$T = 400\text{ K}$	$E_{intra/mer}$ (kJ/mol)	41.3 \pm 0.2	43.0 \pm 0.1	43.3 \pm 0.2	43.6 \pm 0.2	43.7 \pm 0.1
	E_{coh} (MJ/mol)	80.3 \pm 0.2	64.8 \pm 0.2	49.6 \pm 0.2	48.6 \pm 0.2	50.8 \pm 0.3
	e_{coh} (MPa)	608 \pm 2	445 \pm 2	393 \pm 2	360 \pm 2	360 \pm 2
	δ_h (MPa ^{1/2})	24.65 \pm 0.04	21.10 \pm 0.04	19.83 \pm 0.04	18.98 \pm 0.04	19.0 \pm 0.05
$T = 500\text{ K}$	$E_{total/mer}$ (kJ/mol)	52.6 \pm 0.2	55.3 \pm 0.2	55.6 \pm 0.2	55.7 \pm 0.2	55.9 \pm 0.2
	$E_{intra/mer}$ (kJ/mol)	80.7 \pm 0.2	75.6 \pm 0.2	74.0 \pm 0.3	71.7 \pm 0.2	72.4 \pm 0.2
	E_{coh} (MJ/mol)	72.7 \pm 0.4	58.3 \pm 0.3	46.1 \pm 0.6	42.6 \pm 0.4	46.1 \pm 0.3
	V (nm ³)	230.8	254.0	219.6	234.1	244.9
	e_{coh} (MPa)	523 \pm 3	381 \pm 2	349 \pm 4	303 \pm 3	312 \pm 2
	δ_h (MPa ^{1/2})	22.87 \pm 0.06	19.53 \pm 0.05	18.67 \pm 0.11	17.39 \pm 0.08	17.68 \pm 0.06

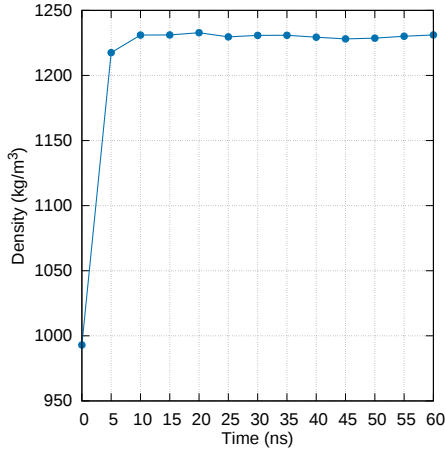


Figure S 2: Time evolution of the density of the 156-PLGA sample averaged every 5 ns of NPT-MD at T=500 K and 1 atm.

3-regression optimized fit for obtaining the $T_{g\alpha}$ and $T_{g\beta}$. Figure S4 provides the same calculation for the BCC case.

4. Structural properties

Figure S5 illustrates the atomic radial distribution functions for the six different atom pairs in the PLGA(50:50) samples.

5. Properties of the individual PLGA(50:50) chains

Figures S5, S6, and S7 illustrate the distributions of the radius of gyration, the end-to-end distance and the SASA from the 20 ns MD-NVE simulations at T= 300 K and T=500 K and their corresponding equilibrium densities for the BCC case. To be note is that these distributions are not normal and have a wide spread. The distributions for the RESP case were very similar to the ones shown for the BCC case.

Figure S9 shows the radial distribution function $g(r)$ of the intra-chain distances between monomers center or mass of each PLGA chain. These functions

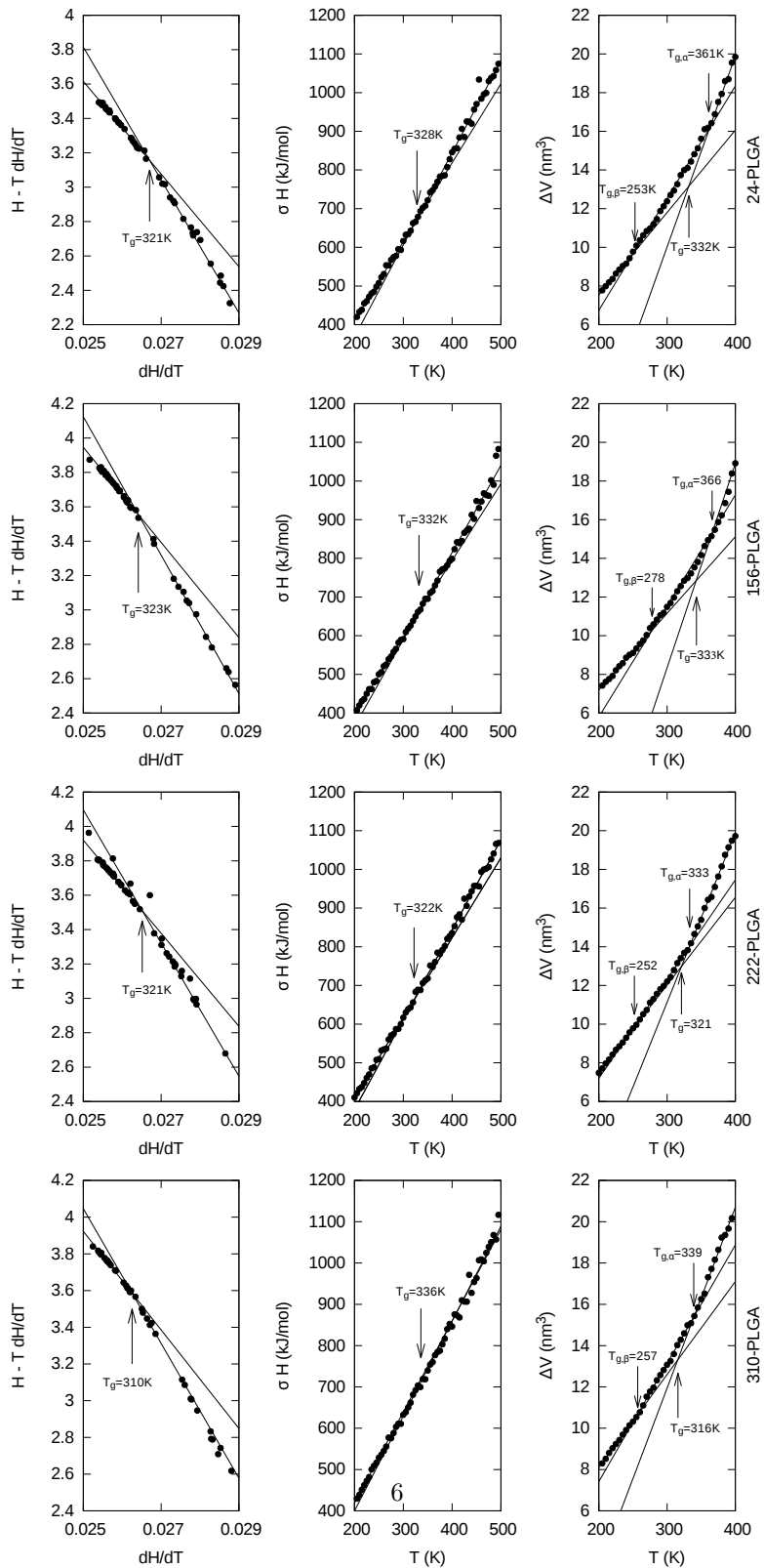


Figure S 3: RESP case data employed for determining T_g , T_{g_α} and T_{g_β}

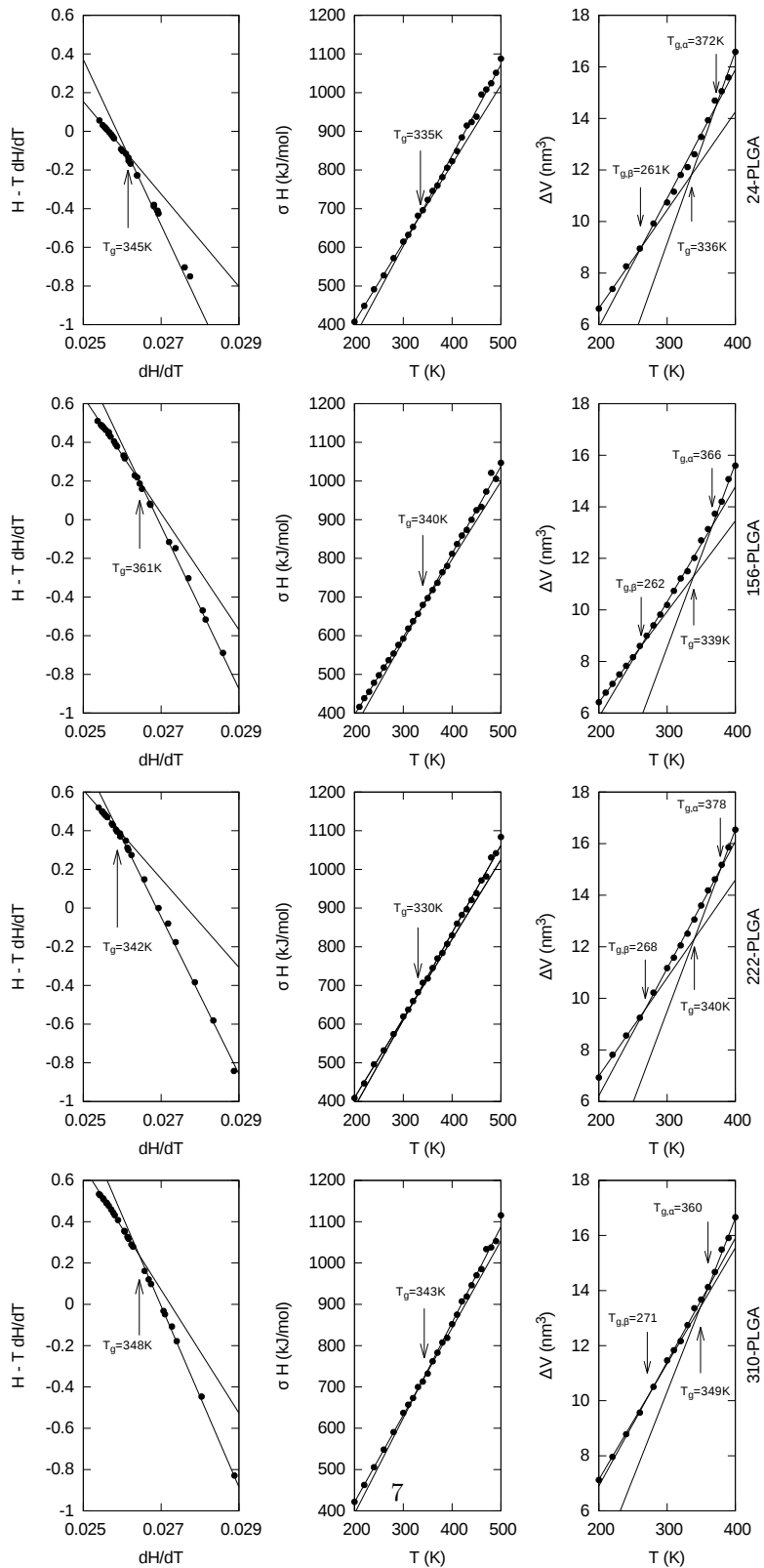


Figure S 4: BCC case data employed for determining T_g , $T_{g\alpha}$ and $T_{g\beta}$

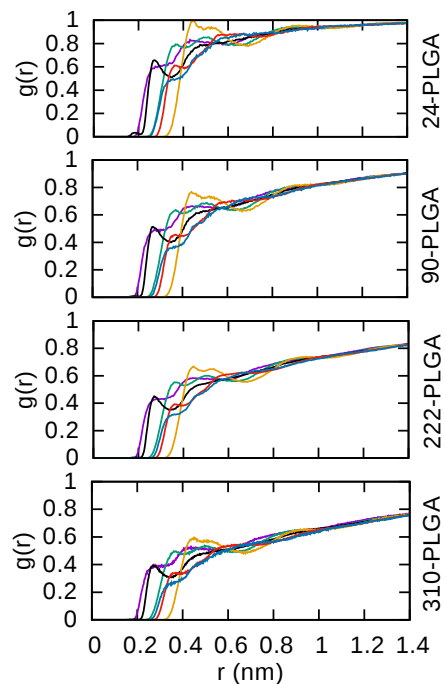


Figure S 5: Radial distribution functions based on distances between the different pairs of atoms belonging to different polymer chains at $T = 300$ K and the density of each PLGA sample. Color scheme is: OH (black), CC (orange), CO (red), OO (blue), CH (green), HH(violet).

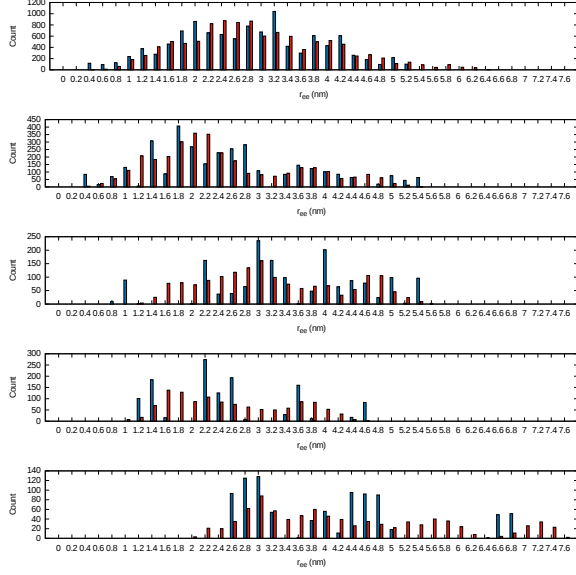


Figure S 6: Distribution of the end-to-end distance, r_{ee} at $T = 300$ K (blue) and $T=500$ K (red) along 20 ns of MD-NVE simulations for the BCC case.

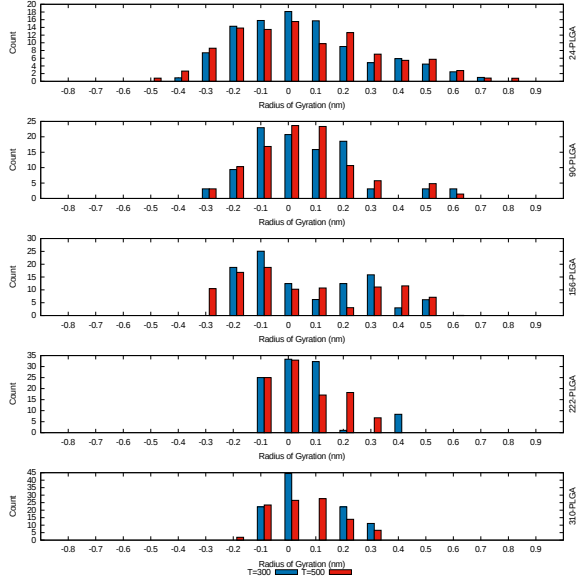


Figure S 7: Distribution of the radius of gyration at $T = 300$ K (blue) and $T=500$ K (red) along 20 ns of MD-NVE simulations for the BCC case.

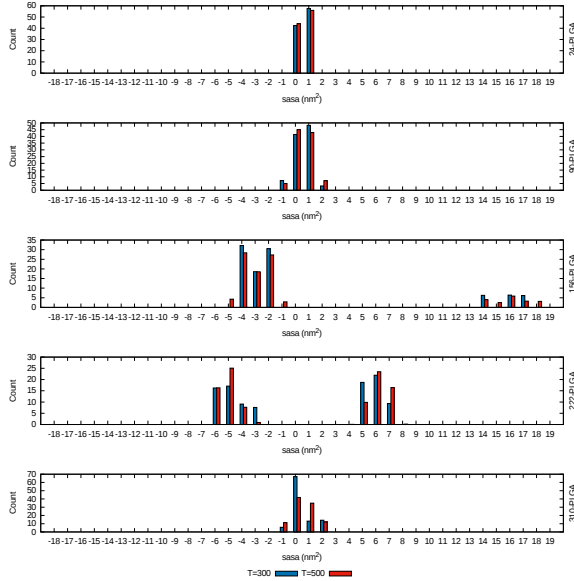


Figure S 8: Distribution of the SASA at $T = 300$ K (blue) and $T = 500$ K (red) along 20 ns of MD-NVE simulations for the BCC case

are normalized by a factor that yields a decaying exponential envelope to be one at $r=0$.

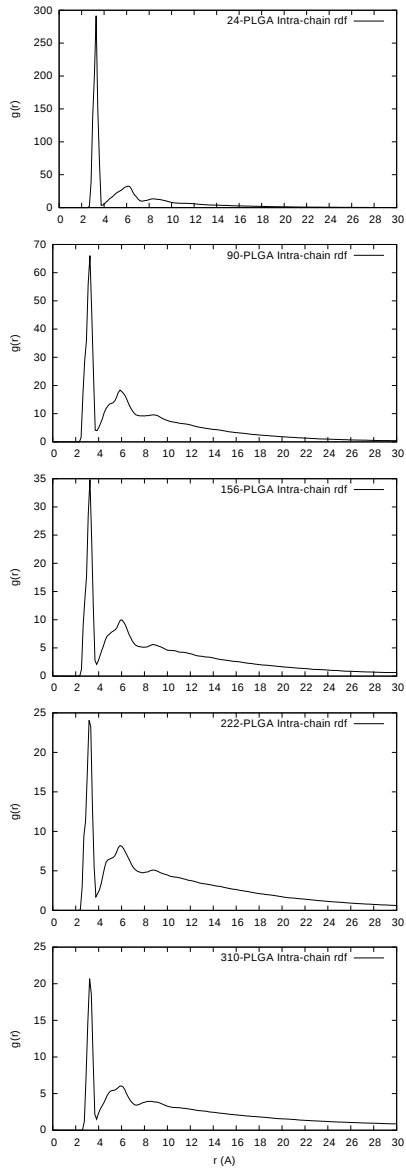


Figure S 9: Radial distribution function of distances between monomers within the polymer chains T= 300 K. Values presented correspond to averages over all the chains in each sample and over 20 ns of NVE MD at 300 K and the corresponding density of each system.